PHYSICAL REVIEW B **93**, 024424 (2016)

Relaxation dynamics in the frustrated Cr_9 antiferromagnetic ring probed by NMR

E. Garlatti,[1] S. Bordignon,[1] S. Carretta,[1] G. Allodi,[1] G. Amoretti,[1] R. De Renzi,[1] A. Lascialfari,[2] Y. Furukawa,[3] G. A. Timco,[4] R. Woolfson,[4] R. E. P. Winpenny,[4] and P. Santini[1]

[1]*Dipartimento di Fisica e Scienze della Terra, Università di Parma, Parco Area delle Scienze 7/A, 43124 Parma, Italy*

[2]*Dipartimento di Fisica, Università degli Studi di Milano and INSTM unit, Via Celoria 16, 20133 Milano, Italy*

[3]*Department of Physics and Astronomy, Iowa State University, Ames, Iowa 50011, USA*

[4]*School of Chemistry and Photon Science Institute, University of Manchester, Oxford Road, Manchester M13 9PL, United Kingdom*

(Received 5 October 2015; revised manuscript received 11 December 2015; published 29 January 2016)

We investigate the magnetic properties and the phonon-induced relaxation dynamics of the first regular Cr_9 antiferromagnetic (AF) ring, which represents a prototype frustrated AF ring. Geometrical frustration in Cr_9 yields an energy spectrum with twofold degenerate low-lying levels and a low-spin ground state. The electronic relaxation dynamics is probed by ^{1}H-NMR through the temperature dependence of the spin-lattice relaxation rate $1/T_1$. We develop a microscopic model that reproduces $1/T_1(T)$ curves, taking also into account the wipeout effect. By interpreting these measurements we determine the spin-phonon coupling strength and we investigate the decay of the cluster magnetization due to the spin-phonon interaction. We find that at very low temperatures, the relaxation is characterized by a single dominating Arrhenius-type relaxation process, whereas several relevant processes emerge at higher temperatures. In addition, we calculate the temperature and magnetic field dependence of level lifetimes.

DOI: 10.1103/PhysRevB.93.024424

I. INTRODUCTION

Molecular nanomagnets (MNMs) [1] are spin clusters whose magnetic interactions can be engineered at the synthetic level. Being among the first examples of real spin systems of finite size, they are at the forefront of research in condensed-matter physics and constitute test beds for fundamental concepts in quantum mechanics. Sophisticated experiments and targeted research activities have unveiled a variety of fundamental quantum phenomena [2] and of potential technological applications [3]. One of the most important goals is to reach a deep understanding of the relaxation dynamics of MNMs, because this aspect is of paramount importance in the design of new molecules acting as classical or quantum bits. One of the most important classes of MNMs is that of even-membered antiferromagnetic (AF) rings, where the metal ions form almost perfect regular polygons. These systems are characterized by a highly nonclassical $S = 0$ ground state (**S** being the total spin of the molecule) and can display quantum tunneling of the Néel vector [4,5], which is the AF counterpart of magnetization tunneling. These systems have been also exploited to investigate the nature of the elementary excitations in finite AF systems [5,6]. One of the most studied AF rings is Cr_8 [7], which is formed by eight AF-coupled Cr^{3+} ions ($s = 3/2$) [6–8]. Heterometallic rings with a magnetic ground state can be obtained from homonuclear ring by chemical substitution of one or two magnetic centers. In particular, Cr_7M rings (M = Zn, Cd, Mn, Ni) are derived from Cr_8 by substitution of one divalent cation M for a trivalent Cr ion [9]. Among them, Cr_7Ni has been shown to be an excellent candidate to encode qubits [2,10–13]. In addition, magnetically open AF rings like Cr_8Cd are reference systems to study the microscopic magnetic behavior of finite AF chains [14].

The attention is now focusing on the last missing members of the AF rings family: closed rings with an odd number of magnetic ions. This kind of molecules is very important because they can be considered as model systems for frustration-induced properties. Indeed, if these rings have a regular geometry and half-integer local spins, they obey the definition of *degenerate frustration* given by O. Kahn [15], displaying a degenerate pair of $S = 1/2$ doublets as ground states. However, sizable structural distortions in the geometry of these molecular polygons lead to the removal of frustration and thus of the degeneracy in the ground state, even if there are still competing AF interactions [15]. The simplest odd-numbered molecular AF rings are AF triangles like Cu_3 [16], whereas larger rings have been much more challenging to synthesize. The first example of AF ring with $N = 9$ is Cr_8Ni [17,18], which, however, is not frustrated because the Ni^{2+} ion breaks the nonagonal symmetry. Another interesting molecule is the $\{VO\}_7$ [19] ring, which has been characterized only by low-temperature dc magnetization measurements. Recently, the first examples of Cr_9 rings have been synthesized and studied [20–22], but none of them displays the characteristics of a degenerate-frustrated ring. Indeed, they all have at least one significant bond defect, leading to a sizable removal of the degeneracy in the $S = 1/2$ ground state or even to a ground state with $S > 1/2$.

In this paper, we study the first regular Cr_9 AF ring (of formula $C_{90}H_{162}Cr_9F_9O_{36}$ [23]), which represents a prototype of a practically degenerate-frustrated homometallic ring. In this compound all the Cr-Cr edges are bridged in the same manner, by one fluoride and two pivalate ligands (see Fig. 1) and susceptibility and low-temperature magnetization measurements are very well reproduced by assuming a single exchange constant. Frustration in molecular nanomagnets yields energy spectra with degenerate levels and novel physical properties, which affect their relaxation dynamics [24,25]. While magnetic relaxation in even-membered AF rings like Fe_6 and Cr_8 has already been theoretically and experimentally investigated [26,27], no equivalent experimental or theoretical studies exist on frustrated AF rings.

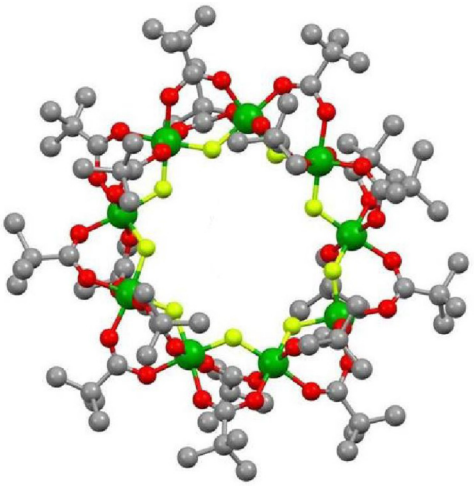

FIG. 1. Molecular structure of Cr_9 crystallized from acetone. Green, Cr; red, O; grey, C; and yellow, F (hydrogen atoms not shown for clarity).

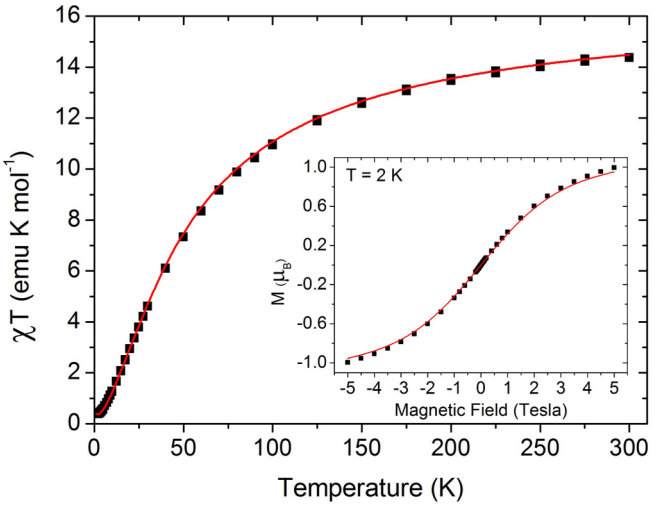

FIG. 2. Measured temperature dependence of χT of Cr_9 (black circles) compared with theoretical calculations (solid line). (Inset) Experimental (squares) and calculated (line) Cr_9 magnetization per molecule at $T = 2$ K as a function of the applied magnetic field. All the calculations are obtained with the Hamiltonian in Eq. (1) and $J = 1.35$ meV and $g = 1.98$.

AF rings are characterized by a relatively fast phonon-induced relaxation. Hence the best technique to probe such dynamics is nuclear magnetic resonance (NMR) [26,28]. Therefore we have investigated Cr_9 by ^{1}H-NMR, by measuring the temperature dependence of the proton spin-lattice relaxation rate $1/T_1(T)$ for different values of the applied magnetic field [26,29]. We have developed a theoretical model for Cr_9 including magnetoelastic couplings which allows us to reproduce $1/T_1$ data, taking also into account the subtle wipeout effect [30]. The interpretation of these measurements has allowed us to estimate the coupling between electron spins and phonons, and to study the decay of the molecular magnetization. We find that Cr_9 is characterized by one dominating Arrhenius relaxation process only at low temperature, whereas several relaxation processes are important above $T = 3$ K. We note in passing that in the ideal case all the corresponding relaxation rates are twofold degenerate, like low-lying energy levels. At last, the so-obtained model allows us to predict the temperature and magnetic field dependence of level lifetimes and to propose a challenging neutron scattering experiment to directly investigate how the frustration is ultimately removed and the resulting low-frequency quantum dynamics.

II. THEORETICAL MODEL

Cr_9 contains nine AF-coupled Cr^{3+} ions ($s = 3/2$). Previously studied Cr_9 molecules have had one significant bond defect, with only one pivalate and one fluoride on one Cr-Cr edge [20,21], leading to a significantly weaker exchange interaction between those two Cr^{3+} ions. The Cr_9 variant studied in this paper, with a formula $Cr_9F_9\{O_2CC(CH_3)_2\}_{18}$ [23] has identical bridging on each edge, with one fluoride and two pivalates present on each edge. The compound has been characterized by mass spectrometry and elemental analysis, and by x-ray diffraction studies. When recrystallized from toluene, crystals are obtained in high yield that form in the hexagonal crystal system. Diffraction studies reveal a nine-metal ring formed about a threefold crystallographic axis; as the organic ligands cannot be arranged with threefold symmetry, the remainder of the structure is highly disordered leading to poor diffraction. Recrystallization of these Cr_9 crystals from acetone or *n*-propanol produces very small crystals in poor yield but which form in a monoclinic or orthorhombic crystal system respectively, which allows a full crystal structure to be obtained (shown in Fig. 1 for crystals grown from acetone). In turn, if these crystals are recrystallized again from toluene, we regain the hexagonal crystals. As Cr_9 is chemically identical in each crystal, we have carried out physical studies on the crystals formed in high yield from toluene. However, to interpret the NMR spectroscopy, we used the full structure obtained on Cr_9 crystallized from acetone to determine the H-atom positions.

Magnetic properties of this regular Cr_9 variant can be described by the following spin Hamiltonian:

$$\mathcal{H}_1 = J \sum_{i=1}^{N} \mathbf{s}_i \cdot \mathbf{s}_{i+1} + g\mu_B \mathbf{B} \cdot \sum_{i=1}^{N} \mathbf{s}_i \qquad (1)$$

($s_i = 3/2$ for Cr^{3+} and $N = 9$ is the number of magnetic ions in the molecule, with the usual cyclic boundary condition $N + 1 = 1$). The first term represents the isotropic Heisenberg exchange interaction, with the same exchange parameter J for all the bonds, and the last one is the Zeeman coupling to an external magnetic field ($g = 1.98$ for Cr^{3+}). Anisotropy effects due to the introduction of a small zero-field splitting term in Eq. (1) are discussed in Sec. V.

We determine the exchange parameter J in Eq. (1) by susceptibility and low-temperature magnetization measurements (Fig. 2). DC SQUID magnetometry on a powdered sample of Cr_9 has been performed on a MPMSXL-5 SQUID magnetometer, in the temperature range of 2–300 K and field range of 0–5 T. The monotonic decrease of χT indicates the presence of dominant AF interactions leading to a low-spin ground state (Fig. 2). Low-temperature magnetization data

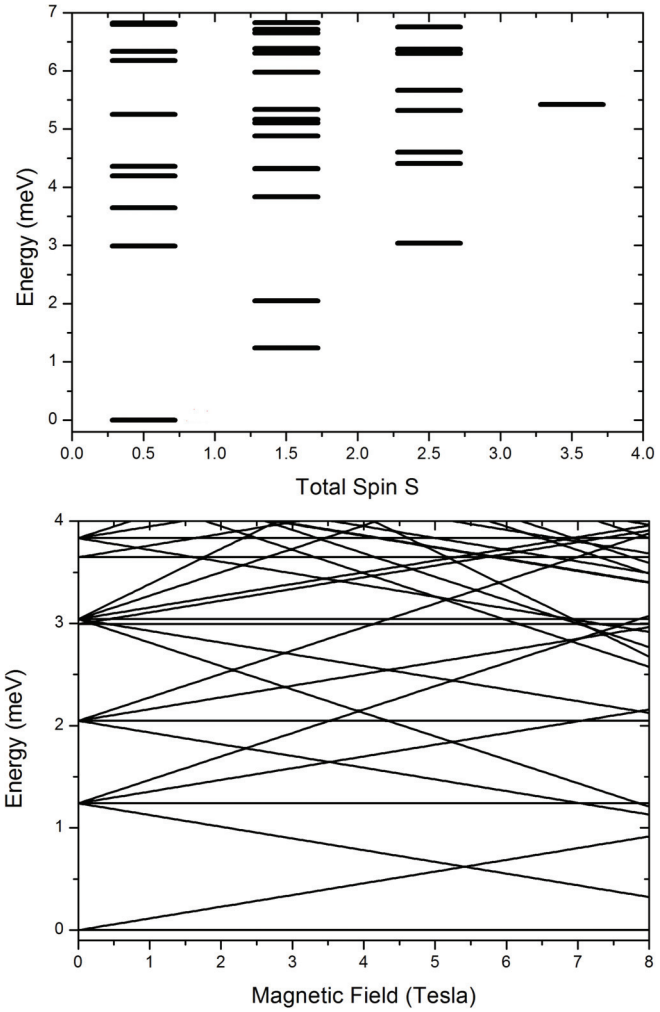

FIG. 3. (Top) Spectrum of (1) for $J = 1.35$ meV and $B = 0$. Energy levels are arranged into multiplets of given total spin S with degeneracy $2S + 1$. The lowest total-spin multiplets are degenerate because of frustration. (Bottom) Magnetic field dependence of the lowest lying energy levels of Cr_9. The ground-state energy is set to zero for each value of B.

saturate to $1\mu_B$ per molecule (inset of Fig. 2). This value of the magnetization per molecule points to a $S = 1/2$ ground state at least up to 5 T, being $g = 1.98$. Figure 2 shows that magnetic measurements can be well reproduced by the model Hamiltonian in Eq. (1) with a single AF exchange coupling $J = 1.35$ meV. Within this model, the Cr_9 molecule has a perfect C_9 symmetry and therefore geometrical frustration. Indeed, the lowest-energy multiplets in the spectrum (Fig. 3, top panel) are twofold degenerate. In particular, the energy gap between the $S = 1/2$ ground manifold and the first excited multiplets with $S = 3/2$ is $\Delta_{01} = 1.2$ meV. The calculated magnetic field dependence of the low-lying energy levels is displayed in Fig. 3.

Irreversible relaxation dynamics in MNMs is caused by the interaction of electronic spins with phonons, behaving like a heat bath. With the formalism of master equations, we can describe the time evolution of the molecular observables and the decoherence phenomena induced by electron spin-phonon interactions [26]. Since NMR measurements typically probe only the quasielastic spectral contribution to the electronic spin dynamics [26,31], we focus on the time evolution of the population $p_s(t)$ of each eigenstate $|s\rangle$ of (1), given by the master equations:

$$\dot{p}_s = \sum_t W_{st}\, p_t. \tag{2}$$

W_{st} is an element of the rate matrix $\mathbb{W}$, i.e., the probability per unit time that a transition between the eigenstates $|t\rangle$ and $|s\rangle$ is induced by the interaction with the phonon heat bath. Here, we assume that each magnetic ion experiences a spherically symmetric magnetoelastic coupling with the surrounding atoms. Thus we can write the transition rates as [32]

$$W_{st} = \gamma^2\pi^2\Delta_{st}^3 n_{ph}(\Delta_{st}) \times \sum_{i,j=1}^{N} \sum_{q_1,q_2=x,y,z} \langle s|O_{q_1,q_2}(\mathbf{s}_i)|t\rangle\langle s|O_{q_1,q_2}(\mathbf{s}_j)|t\rangle^*, \tag{3}$$

where $n_{ph}(x) = (e^{\hbar x/k_B T} - 1)^{-1}$, $\Delta_{st} = (E_s - E_t)/\hbar$ and $O_{q_1,q_2}(\mathbf{s}_i) = (s_i^{q_1} s_i^{q_2} + s_i^{q_2} s_i^{q_1})/2$ are the quadrupolar operators. The coupling strength γ is the only free parameter [33] and it can be determined from NMR experimental data [25,28].

The study of dynamical correlation functions of the fluctuations of molecular observables $\mathcal{S}_{\mathcal{P},\mathcal{Q}}(t) = \langle(\mathcal{P}(t) - \mathcal{P}_{eq})(\mathcal{Q}(t) - \mathcal{Q}_{eq})\rangle$ allow us to understand the relaxation dynamics of MNMs, where $\mathcal{P}$ and $\mathcal{Q}$ are molecular observables defined by spin operators acting on the electronic spins of the system (*e.g.* magnetization $\mathcal{M} = \sum_i s_i$). In our theoretical framework, the Fourier transform of the correlation function is expressed as a sum of Lorentzians [26]:

$$\mathcal{S}_{\mathcal{P},\mathcal{Q}}(\omega) = \sum_{i=1}^{n} A(\lambda_i, T, B)\frac{\lambda_i(T,B)}{\lambda_i(T,B)^2 + \omega^2} \tag{4}$$

(n is the dimension of the Hilbert space). The relaxation rates λ_i are the eigenvalues of $-\mathbb{W}$ and they are the inverse of the characteristic relaxation times $\tau_{\rm rel}^{(i)} = 1/\lambda_i$. The weights $A(\lambda_i, T, B)$ of each rate λ_i are calculated by Eqs. (2) and (3), as explained in Ref. [26,34].

III. NMR AS A PROBE OF RELAXATION DYNAMICS

Phonon-induced relaxation dynamics in AF rings is characterized by fast relaxation times $\tau_{\rm rel}^{(i)}$, which can be probed by the proton spin-lattice relaxation rate $1/T_1$, measured by NMR. In fact, thermal fluctuations of the electronic spins generate fluctuations in the local hyperfine fields at the nuclear sites, causing relaxation of the nuclear spins. ^{1}H pulsed NMR experiments are performed on powdered samples of Cr_9 by means of a HyReSpect NMR spectrometer [35], at several applied magnetic fields and in the temperature range 2–100 K. The ^{1}H nuclear spin-lattice relaxation rate $1/T_1$ is determined by monitoring the recovery of the longitudinal nuclear magnetization after the full irradiation of the nuclear absorption line, using a comb of radiofrequency pulses followed by a $\pi/2 - \pi/2$ solid-echo sequence.

The theoretical model of Sec. II allows one to interpret also ^{1}H-NMR experiments. By the same density matrix formalism

used for the electron spin-phonon coupling, we can describe an ensemble of protons in an external static magnetic field, coupled to the perturbative fluctuating field produced by electronic spins. We follow the theory of relaxation processes of Redfield (for futher details see Refs. [25,36,37]) and we calculate the spin-lattice $\frac{1}{T_1}$ and the spin-spin $\frac{1}{T_2}$ relaxation rates taking as inputs the positions of the magnetic ions and protons in the molecule:

$$\frac{1}{T_1} = \sum_{\substack{i,j=1,N \\ p,p'=x,y,z}} C_{i,j}^{p,p'} \left[\mathcal{S}_{s_i^p, s_j^{p'}}(\omega_L) + \mathcal{S}_{s_i^p, s_j^{p'}}(-\omega_L) \right], \quad (5)$$

$$\frac{1}{T_2} = \frac{1}{2T_1} + \sum_{\substack{i,j=1,N \\ p,p'=x,y,z}} K_{i,j}^{p,p'} \left[\mathcal{S}_{s_i^p, s_j^{p'}}(0) \right], \quad (6)$$

where the $C_{i,j}^{p,p'}$ and $K_{i,j}^{p,p'}$ are geometric coefficients of the hyperfine dipolar interaction between magnetic ions and protons [28].

Since Cr_9 is a homometallic regular ring, $\frac{1}{T_1}$ measurements can be used to directly probe the relaxation of the cluster magnetization [26]. Indeed, for each eigenstate $|t\rangle$ $\langle t|s_i^p|t\rangle = \langle t|s_j^p|t\rangle = \frac{1}{N}\langle t|S_p|t\rangle$, where $S_p = \sum_i s_i^p$ is the p component of the *total* spin operator. Then (5) and (6) become

$$\frac{1}{T_1} = \sum_{p,p'=x,y,z} G_{p,p'} \left[\mathcal{S}_{S_p, S_{p'}}(\omega_L) + \mathcal{S}_{S_p, S_{p'}}(-\omega_L) \right], \quad (7)$$

$$\frac{1}{T_2} = \frac{1}{2T_1} + \sum_{p,p'=x,y,z} J_{p,p'} \left[\mathcal{S}_{S_p, S_{p'}}(0) \right], \quad (8)$$

where the $G_{p,p'}$ and $J_{p,p'}$ are geometrical coefficients depending only on the positions of the spins and of the probed nuclei [38].

IV. NMR RESULTS

The temperature-dependence of the spin-lattice relaxation rate $1/T_1$ is shown in Fig. 4, normalized to χT, which is proportional to the size of equilibrium fluctuations. $(1/T_1)/(\chi T)$ displays a peak at 10 K when $B = 0.55$ T, which lowers and moves to higher temperatures by increasing the field. The bottom panel of Fig. 4 shows that Cr_9 deviates from the Bloembergen-Purcell-Pound (BPP) behavior, i.e., the height of the peaks in $(1/T_1)/(\chi T)$ for different values of B does not scale exactly as $1/B$. The BPP behavior has been observed in the even-numbered homometallic ring Cr_8 (see inset of Fig. 4) and other nanomagnets [26,31], whose dynamics is characterized by a single dominating relaxation rate λ_0. Hence this suggests the presence of more than one relevant relaxation frequency in the temperature range where $(1/T_1)/(\chi T)$ displays a peak, even if Cr_9 is homometallic. The origin of the peak in the temperature-dependence of $(1/T_1)/(\chi T)$ can be understood by using (4) to rewrite the Fourier transforms of the correlation functions at the Larmor frequency $\mathcal{S}_{S_p, S_{p'}}(\pm\omega_L)$ of Eq. (7). As mentioned above, in the case of homometallic AF rings only a single lorentzian dominates the sum in Eq. (4) [26,31] and $(1/T_1)/(\chi T)$ displays a peak at the temperature at which the relaxation rate of this lorentzian matches ω_L. If the relaxation dynamics is not mono-lorentzian but the different relevant rates are close to one another when they approach ω_L, we have again a single peak in the $(1/T_1)/(\chi T)$ [25,28]. Thus Cr_9 NMR data point to this second situation.

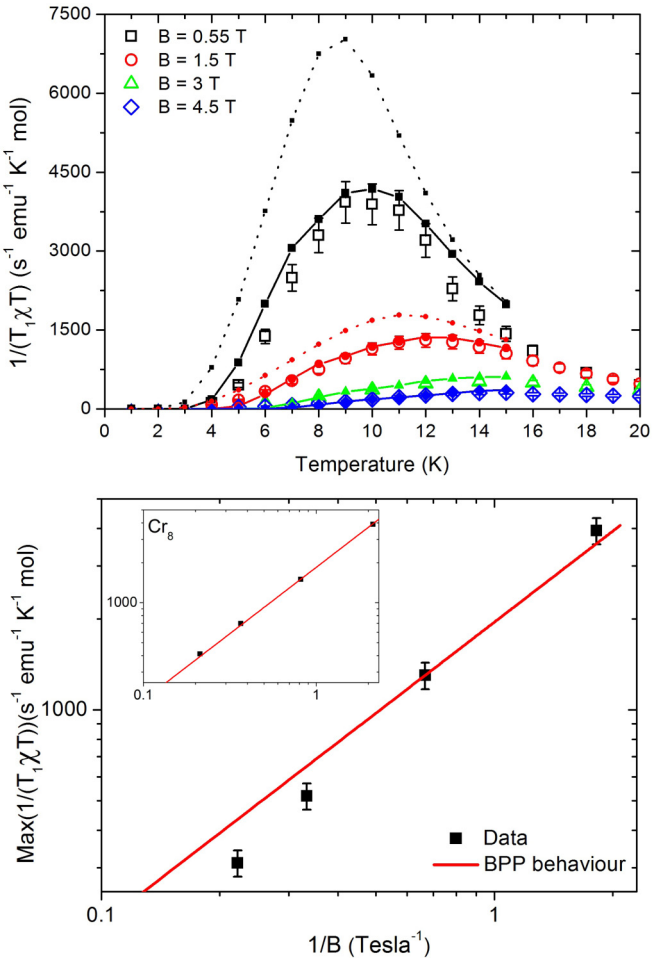

FIG. 4. (Top) ^{1}H NMR $(1/T_1)/(\chi T)$ data on Cr_9 powders as a function of temperature at four different applied magnetic fields (scatter) and calculations exploiting equation (5) and taking into account the wipeout effect (line&scatter). Dashed line and scatter for $B = 0.5$ and 1.5 T represent calculations of $(1/T_1)/(\chi T)$ with no wipeout effect. (Bottom) Experimental height of the peaks of $(1/T_1)/(\chi T)$ of Cr_9 for the four different values of the inverse magnetic field (scatter), compared with the BPP behavior, determined by taking as a reference the data at $B = 1.5$ T (solid line). (Inset) Experimental peaks of $(1/T_1)/(\chi T)$ for Cr_8 [31], compared with the BPP behavior, determined by taking as a reference the data at $B = 1.23$ T.

Experimental data are interpreted within the theoretical framework illustrated in Secs. II and III. By fitting the position of the peak in temperature, it is possible to determine the spin-phonon coupling strength γ. The presence of a peak at 10 K in the $(1/T_1)/(\chi T)$ curve of Cr_9 with $B = 0.55$ T yields $\gamma = 4 \times 10^{-4}$ THz^{-1}. With the same γ it is possible to reproduce the position and height of the peaks of $(1/T_1)/(\chi T)$ also for the other values of B (1.5, 3, and 4.5 T). Thus we obtain a good overall quantitative agreement between data and calculations (Fig. 4), in spite of the complexity of the NMR

technique applied to this kind of systems. Furthermore, the value of γ found for Cr_9 is similar to that of other related AF ring like Cr_7Ni and Cr_8 ($\gamma = 2.8 \times 10^{-4}$ THz^{-1}) [28]. Since measurements have been made on powders, to reproduce the experimental data we average over all the possible orientations of the applied magnetic field. To reduce the computational effort in the diagonalization of the rate matrix $\mathbb{W}$, it is necessary to truncate the molecule Hilbert space. The reduction to the subspace spanned by the total-spin manifolds up to 150 K allows us to reproduce the temperature dependence of $(1/T_1)/(\chi T)$ in the most interesting region, i.e., where it displays a peak, up to $T = 15$ K. Anyway this truncation leads to a slight overestimate of the calculated $(1/T_1)/(\chi T)$ with respect to the corresponding experimental values for $T > 12$ K [39].

^{1}H NMR measurements are often affected by the so-called wipeout effect. It consists of a signal loss in the NMR signal intensity, due to the enhancement of the transverse relaxation rates $1/T_2$ of the protons over the limit fixed by the experimental setup (around 67–100 (ms)$^{-1}$ in our experimental conditions, corresponding to $T_2 \sim 10$–15 μs) [30]. Thus, to calculate the spin-lattice relaxation rate of Cr_9, we take into account also the wipeout effect. For each hydrogen, we calculate $1/T_1$ and $1/T_2$ as a function of the temperature, the orientation and the modulus of the applied magnetic field with (7) and (8). Then we retain only the hydrogen nuclei whose transverse relaxation rate is lower than the above-mentioned threshold. In order to obtain the $(1/T_1)/(\chi T)$ curves of Cr_9 in Fig. 4, we set $1/T_2^{\text{thresh}} = 81.7$ (ms)$^{-1}$, corresponding to $T_2^{\text{thresh}} = 12.2$ μs. This approach has already been applied to reproduce the wipeout effect in the Fe_7 cluster, yielding very good results [25]. Furthermore, the comparison between experimental data and calculations of $(1/T_1)/(\chi T)$ performed retaining all the protons in the molecule (dashed line and scatter in Fig. 4, top panel) shows the extent of the signal loss due to the wipeout effect, which is, as expected, stronger at low fields. Thus we can conclude that the wipeout effect is a crucial ingredient in the interpretation of ^{1}H NMR experimental data.

As a test, we have also measured the transverse nuclear magnetization $M_{xy}^H(0)$, obtained by the extrapolation at zero time of the transverse nuclear magnetization $M_{xy}^H(t)$ recovery curve. The quantity $M_{xy}^H(0)T$, where T is the temperature, is proportional to the number of protons resonating at the irradiation frequency. Transverse nuclear magnetization measurements as a function of temperature have been performed at $B = 0.55$ T since wipeout is generally stronger at small fields (see also Fig. 4, top panel). $M_{xy}^H(0)T$, and thus the number of probed protons, decreases by lowering the temperature due to the wipeout effect [30]. In Fig. 5, we compare the number of protons in Cr_9 probed by NMR measurements with the number of ^{1}H nuclei included in our calculations by the method described above. The graph shows that with our calculations it is possible to reproduce the wipeout effect, confirming the reliability of our model.

The bottom panel of Fig. 3 shows that we predict a level crossing between the first and the second excited levels of Cr_9 at about 5.4 T. At the level crossings there is a strong increase of both $1/T_1$ and $1/T_2$ due to inelastic contributions to the relaxation dynamics, thus we expect a strong wipeout

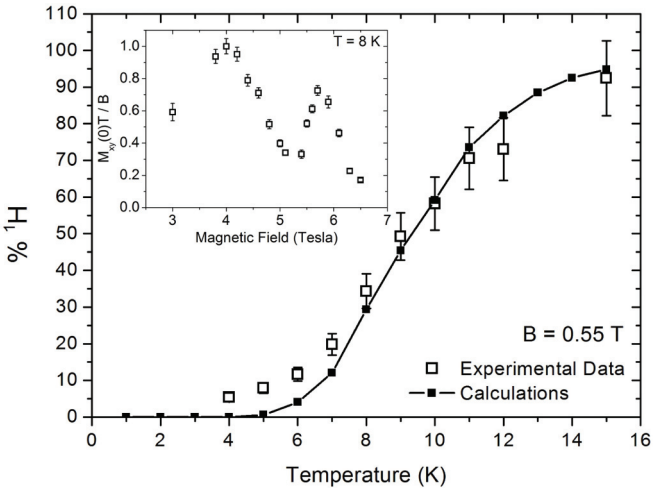

FIG. 5. Fraction of protons probed by NMR (black) deduced by the initial transverse nuclear magnetization at $B = 0.55$ and 1.5 T (see Sec. III) compared with fraction of protons taken into account in our calculations (red and blue) determined as described in Sec. IV. (Inset) Renormalized transverse nuclear magnetization $M_{xy}^H(0)T/B$ as a function of the applied magnetic field B at $T = 8$ K. Data have been also renormalized so that the maximum value of the magnetization in the explored magnetic fields range is set to 1.

effect [40]. We have therefore measured $M_{xy}^H(0)T$ as a function of the applied magnetic field at $T = 8$ K, in order to populate the lowest excited levels involved in the crossing. Experimental data are shown in the inset of Fig. 5. As expected, the transverse nuclear magnetization displays a minimum between 5 and 5.5 T, indicating a strong wipeout effect and confirming the level crossing field.

V. RELAXATION DYNAMICS

From the analysis of the NMR data we have determined the unique free parameter in Eq. (3), the electron spin-phonon coupling strength γ. Thus we can investigate the relaxation dynamics of the Cr_9 cluster by studying the spectrum of fluctuations of the cluster magnetization M with Eq. (4) ($\mathcal{P} = \mathcal{Q} = \mathcal{M} = \sum_i s_i$).

Figure 6 report the calculated weight $A(T, B; \lambda_i)$ of the characteristic relaxation rates λ_i of the autocorrelation of M [see Eq. (4)], as a function of the inverse temperature. It is worth to stress that γ merely fixes the relaxation timescale (a variation of γ only produces rigid vertical shifts in Fig. 6).

Between 2 and 20 K the relaxation rates $\lambda_i(T)$ are roughly in the range between 10^{-8}–10^{-3} THz. Figure 6 shows that the decay of magnetization in Cr_9 is characterized by a single time only for very low temperatures, even for small applied fields. Indeed, above $T \simeq 3$ K, several relevant relaxation rates emerge. In particular, in the temperature range $10 \lesssim T \lesssim 15$ K, where the relaxation rates intersect the proton Larmor frequencies ω_L (see the red lines in Fig. 6), there are several rates with an appreciable weights, but close to one another. This explains why a single peak in the $(1/T_1)/(\chi T)$(T) is observed in spite of the multitime relaxation dynamics. Only below $T \simeq 3$ K there is a single relaxation process, whose T dependence follows the Arrhenius law.

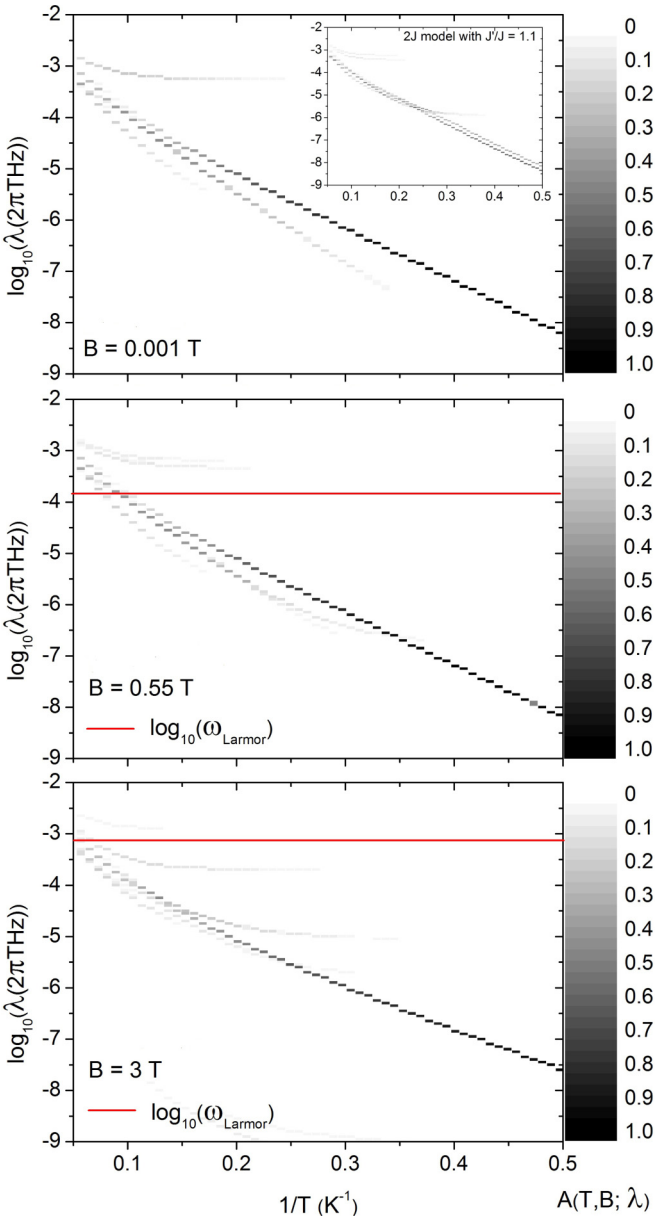

FIG. 6. Intensity plot showing the calculated weights $A(T,B;\lambda_i)$ of the magnetization autocorrelation vs $1/T$ (x axis) for $B = 0.001$, $B = 0.55$, and 3 T respectively. The y axis is $\log_{10}(\lambda_i)$ (in 2πTHz). The plot maps $A(T,B;\lambda_i)/\chi T$, i.e., for each value of T the spectra have been normalized by χT, which is proportional to the size of equilibrium fluctuations. When the rates λ_i with significant weight intersect ω_L (red line), $1/T_1$ displays a peak (see Fig. 4). (Inset) Intensity plot of the calculated weights $A(T,B;\lambda_i)$ vs $1/T$ for $B =$ 0.001 T obtained with a $2J$ model Hamiltonian with $J'/J = 1.1$.

We have analyzed the dominant relaxation processes by inspecting the eigenvectors and the matrix elements of $\mathbb{W}$. In fact, the former give information about the starting and the final states of the processes and the latter are the transition probabilities. In small fields (Fig. 6) the dominant relaxation rates for $T \lesssim 3$ K involve levels of the two degenerate $S = 1/2$ ground doublets and of the second excited $S = 3/2$ multiplets with $E = 23.7$ K (see Fig. 7, blue arrow). They correspond to an Orbach process [41] following the Arrhenius law with an

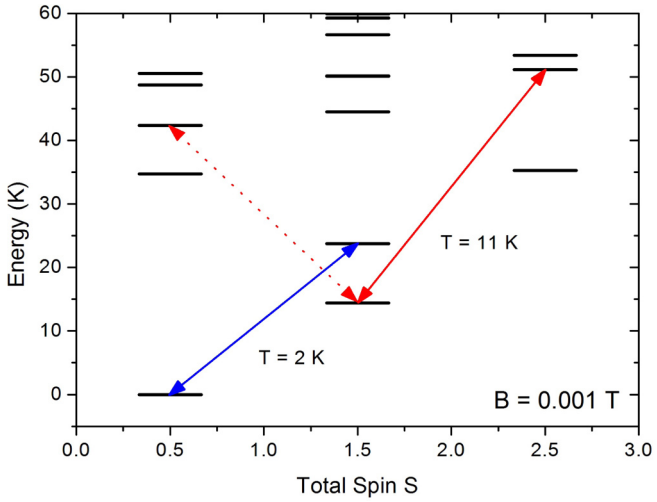

FIG. 7. Relaxation paths corresponding to the dominant relaxation rates λ_i of Cr_9 with $B \to 0$ in the low-temperature regime ($T = 2$ K, blue arrows) and with $T = 11$ K (red arrows).

energy barrier $\Delta/k_B \approx 24$ K, which is the dominant one up to $T \cong 7$ K. At about $T = 3$ K there is a second rate whose weight becomes relevant in the relaxation dynamics, corresponding to a process from the two degenerate first excited multiplets with $S = 3/2$ and $E = 14.4$ K towards higher excited levels with $S = 1/2$ and $5/2$. At higher temperatures ($T > 7$ K, close to the $1/T_1$ peak temperature), these processes become the dominant ones (red arrows in Fig. 7). The presence of an applied magnetic field (see Figs. 6) leads to a faster relaxation, especially at low T. Anyway, the dynamics still have a multiple-times character above 3 K and the relevant relaxation paths always involve the same total-spin multiplets, even if split by the Zeeman interaction.

By comparing the relaxation dynamics of Cr_9 with that of the even-membered parent compound Cr_8 [26], we find that both clusters are characterized by one dominating Arrhenius process at low temperatures, but in Cr_9, additional relaxation processes emerge at significantly lower temperatures than in Cr_8. In addition, within the present model the relevant relaxation rates $\lambda_i(T)$ in Cr_9 are twofold degenerate, reflecting the symmetry of Eqs. (1) and (3). These degeneracies are in fact a peculiar characteristic of highly symmetrical frustrated MNMs. For instance, the relaxation dynamics of the frustrated Ni_7 cluster displays a band of almost degenerate and equally weighted frequencies [24]. These degeneracies can be lifted by reducing the symmetry of the Cr_9 molecule. For instance, by assuming that one Cr-Cr bond is different from the others and thus introducing a different exchange coupling $J' = 1.1J$ for this bond, the cluster is still characterized by competing AF interactions, but the degeneracy of the energy levels is removed. In this case, the relaxation dynamics is dominated by two distinct rates even at low temperature (see an inset in Fig. 6), showing the typical behavior of a cluster with competing AF interactions. For instance, in the Fe_7 double-pyramid cluster, which is characterized by many competing AF interactions, we indeed found a multiple-time scale relaxation dynamics at low temperatures [25]. A lifting of these degeneracies would also result from a less symmetric

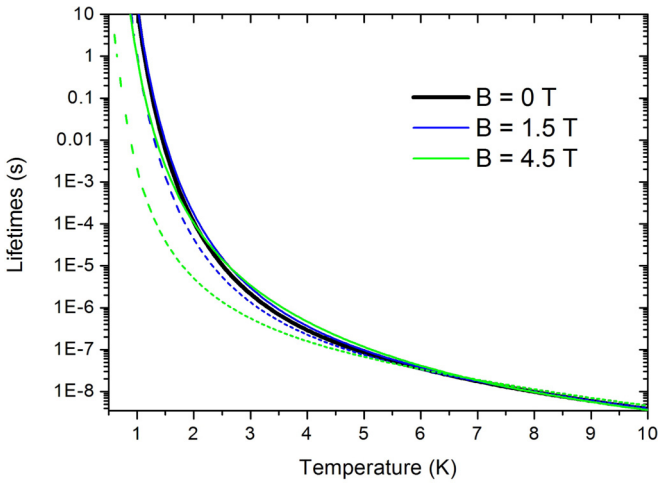

FIG. 8. Calculated temperature-dependence of the lifetime of the levels of the two $S = 1/2$ ground doublets for several values of the applied magnetic field. Continuous and dashed lines correspond to $|S = 1/2, M = -1/2\rangle$ and $|S = 1/2, M = 1/2\rangle$, respectively.

form of the magneto-elastic coupling. Such a coupling would also lead to sizable transition probabilities between the ground manifold and the lowest-energy $S = 3/2$ multiplet, resulting in faster relaxation at very low temperatures. Yet, there is no indication in the present data of a less symmetric model than the one assumed.

The degeneracy between the two $S = 1/2$ ground multiplets and the corresponding perfect frustration is expected to be slightly broken at low temperature because of the Jahn-Teller theorem. A very interesting experiment would be to exploit high-resolution four-dimensional inelastic neutron scattering [42] to study the low-energy peak corresponding to the transition between the two nearly degenerate $S = 1/2$ multiplets. Indeed, the dependence of the intensity of this peak over the momentum transfer vector would yield direct information on how the frustration is removed and on the associated low-frequency quantum dynamics. The spin dynamics associated with this low-energy peak will be damped on a time scale depending on the average of the lifetimes of the involved levels. Hence we use the here-determined model of the magnetic relaxation of Cr_9 to calculate the effect of spin-phonon interaction on the lifetimes of the lowest-energy levels [26]. Figure 8 reports the calculated temperature-dependence of the lifetime of the ground $S = 1/2$ manifold for several values of the magnetic field. At low temperature, the lifetime is very long, making the previously mentioned experiment very promising if large high-quality crystals become available. It is worth to add that direct transitions between the two $S = 1/2$ doublets should not strongly limit the lifetimes, because of the small phonon density associated with a very small energy gap. In addition, Fig. 8 shows that level lifetimes can be also controlled by applying an external magnetic field.

We have also studied the effects of anisotropy on the relaxation properties of Cr_9, by adding a small axial zero-field splitting term to the spin Hamiltonian in Eq. (1) [43,44]. We choose a typical value for the zero-field splitting parameter $d_{Cr} = -0.03$ meV, as the one found in Cr_8 [6–8,42]. The energy levels remain twofold degenerate and thus we still find a pair of degenerate $S = 1/2$ doublets as ground state. We have found that the effect of anisotropy on relaxation is negligible [45]. In particular, the $1/T_1$ curves calculated with anisotropy are very similar to those in the lack of anisotropy, provided the wipeout threshold is reduced from $T_2^{\text{thresh}} = 12.2\ \mu$ to $T_2^{\text{thresh}} = 11.7\ \mu$, still within the dead-time interval fixed by the experimental setup. Thus NMR data can be equally well reproduced with or without the anisotropy term. We have also verified that this term does not affect the relaxation dynamics, as we found find the same temperature and field dependence of the characteristic relaxation rates, which are still twofold degenerate.

VI. CONCLUSIONS

We have investigated the magnetic properties and relaxation dynamics of the first regular Cr_9 AF ring, which represents a prototype of practically degenerate-frustrated homometallic ring of half-integer spins. The energy spectrum of this kind of systems is characterized by a twofold degeneracy of the low-energy total-spin multiplets. The relaxation of Cr_9 has been investigated by measuring the temperature and magnetic field dependence of the spin-lattice relaxation rate $1/T_1$ of ^{1}H nuclei. The experimental results have been interpreted by a microscopic model including magnetoelastic couplings and taking into account the wipeout effect. This model has allowed us to reproduce satisfactorily the experimental results and to study the phonon-induced decay of molecular magnetization. While magnetic relaxation of bipartite rings is well known, this is the first investigation of an odd-membered AF ring. We have found that in Cr_9 the relaxation dynamics is characterized by a single Arrhenius time only at very low temperatures, whereas above 3 K several relevant relaxation rates emerge. In addition, the model predicts the temperature and magnetic field dependence of level lifetimes, which are important for the feasibility of a neutron scattering experiment to directly probe the quantum dynamics resulting from the expected ultimate removal of frustration.

ACKNOWLEDGMENTS

We acknowledge financial support from the FIRB Project No. RBFR12RPD1 of the Italian Ministry of Education and Research. The research was also supported by the US Department of Energy, Office of Basic Energy Sciences, Division of Materials Sciences and Engineering. Ames Laboratory is operated for the US Department of Energy by Iowa State University under Contract No. DE-AC02-07CH11358.

[1] D. Gatteschi, R. Sessoli, and J. Villain, *Molecular Nanomagnets* (Oxford University Press, New York, USA, 2006).

[2] L. Thomas, F. Lionti, R. Ballou, D. Gatteschi, R. Sessoli, and B. Barbara, Nature (London) **383**, 145 (1996); L. Sorace,

W. Wernsdorfer, C. Thirion, A.-L. Barra, M. Pacchioni, D. Mailly, and B. Barbara, Phys. Rev. B **68**, 220407 (2003); P. Santini, S. Carretta, G. Amoretti, T. Guidi, R. Caciuffo, A. Caneschi, D. Rovai, Y. Qiu, and J. R. D. Copley, *ibid.* **71**, 184405 (2005); G. A. Timco, S. Carretta, F. Troiani, F. Tuna, R. J. Pritchard, C. A. Muryn, E. J. L. McInnes, A. Ghirri, A. Candini, P. Santini, G. Amoretti, M. Affronte, and R. E. P. Winpenny, Nat. Nanotech. **4**, 173 (2009); W. Wernsdorfer, N. Aliaga-Alcalde, D. N. Hendrickson, and G. Christou, Nature (London) **416**, 406 (2002); A. Ardavan, O. Rival, J. J. L. Morton, S. J. Blundell, A. M. Tyryshkin, G. A. Timco, and R. E. P. Winpenny, Phys. Rev. Lett. **98**, 057201 (2007); C. Schlegel, J. van Slageren, M. Manoli, E. K. Brechin, and M. Dressel, *ibid.* **101**, 147203 (2008).

[3] R. Sessoli, D. Gatteschi, A. Caneschi, and M. A. Novak, Nature (London) **365**, 141 (1993; L. Bogani and W. Wernsdorfer, Nat. Mat. **7**, 179 (2008); M. Leuenberger and D. Loss, Nature (London) **410**, 789 (2001); E. Garlatti, S. Carretta, J. Schnack, G. Amoretti, and P. Santini, Appl. Phys. Lett. **103**, 202410 (2013).

[4] O. Waldmann, T. C. Stamatatos, G. Christou, H. U. Güdel, I. Sheikin, and H. Mutka, Phys. Rev. Lett. **102**, 157202 (2009).

[5] J. Ummethum, J. Nehrkorn, S. Mukherjee, N. B. Ivanov, S. Stuiber, T. Strässle, P. L. W. Tregenna-Piggott, H. Mutka, G. Christou, O. Waldmann, and J. Schnack, Phys. Rev. B **86**, 104403 (2012).

[6] O. Waldmann, T. Guidi, S. Carretta, C. Mondelli, and A. L. Dearden, Phys. Rev. Lett. **91**, 237202 (2003).

[7] S. Carretta, J. van Slageren, T. Guidi, E. Liviotti, C. Mondelli, D. Rovai, A. Cornia, A. L. Dearden, F. Carsughi, M. Affronte, C. D. Frost, R. E. P. Winpenny, D. Gatteschi, G. Amoretti, and R. Caciuffo, Phys. Rev. B **67**, 094405 (2003).

[8] M. Affronte, T. Guidi, R. Caciuffo, S. Carretta, G. Amoretti, J. Hinderer, I. Sheikin, A. G. M. Jansen, A. A. Smith, R. E. P. Winpenny, J. van Slageren, and D. Gatteschi, Phys. Rev. B **68**, 104403 (2003).

[9] F. K. Larsen, E. J. L. McInnes, H. E. Mkami, J. Overgaard, S. Piligkos, G. Rajaraman, E. Rentschler, A. A. Smith, G. M. Smith, V. Boote, M. Jennings, G. A. Timco, and R. E. P. Winpenny, Angew. Chem. **115**, 105 (2003).

[10] F. Troiani, M. Affronte, S. Carretta, P. Santini, and G. Amoretti, Phys. Rev. Lett. **94**, 190501 (2005).

[11] F. Troiani, A. Ghirri, M. Affronte, S. Carretta, P. Santini, G. Amoretti, S. Piligkos, G. Timco, and R. E. P. Winpenny, Phys. Rev. Lett. **94**, 207208 (2005).

[12] A. Chiesa, G. F. S. Whitehead, S. Carretta, L. Carthy, G. A. Timco, S. J. Teat, G. Amoretti, E. Pavarini, R. E. P. Winpenny, and P. Santini, Sci. Rep. **4**, 7423 (2014).

[13] C. J. Wedge, G. A. Timco, E. T. Spielberg, R. E. George, F. Tuna, S. Rigby, E. J. L. McInnes, R. E. P. Winpenny, S. J. Blundell, and A. Ardavan, Phys. Rev. Lett. **108**, 107204 (2012).

[14] T. Guidi, B. Gillon, S. Mason, E. Garlatti, S. Carretta, P. Santini, A. Stunault, R. Caciuffo, J. van Slageren, B. Klemke, A. Cousson, G. A. Timco, and R. E. P. Winpenny, Nat. Commun. **6**, 7061 (2015).

[15] O. Kahn, Chem. Phys. Lett. **265**, 109 (1997).

[16] B. Cage, F. A. Cotton, N. S. Dalal, E. A. Hillard, B. Rakvin, and C. M. Ramsey, J. Am. Chem. Soc. **125**, 5270 (2003).

[17] O. Cador, D. Gatteschi, R. Sessoli, F. K. Larsen, J. Overgaard, A. Barra, S. J. Teat, G. A. Timco, and R. E. P. Winpenny, Angew. Chem. Int. Ed. **43**, 5196 (2004).

[18] Y. Furukawa, K. Kiuchi, K. I. Kumagai, Y. Ajiro, Y. Narumi, M. Iwaki, K. Kindo, A. Bianchi, S. Carretta, P. Santini, F. Borsa, G. A. Timco, and R. E. P. Winpenny, Phys. Rev. B **79**, 134416 (2009).

[19] N. Hoshino, M. Nakano, H. Nojiri, W. Wernsdorfer, and H. Oshio, J. Am. Chem. Soc. **131**, 15100 (2009).

[20] M. L. Baker, G. A. Timco, S. Piligkos, J. S. Mathieson, H. Mutka, F. Tuna, P. Kozowski, M. Antkowiak, T. Guidi, T. Gupta, H. Rath, R. J. Woolfson, G. Kamieniarz, R. G. Pritchard, H. Weihe, L. Cronin, G. Rajaraman, D. Collison, E. J. L. McInnes, and R. E. P. Winpenny, PNAS **109**, 19113 (2012).

[21] M. Antkowiak, P. Kozlowski, G. Kamieniarz, G. A. Timco, F. Tuna, and R. E. P. Winpenny, Phys. Rev. B **87**, 184430 (2013).

[22] G. Kamieniarz, W. Florek, and M. Antkowiak, Phys. Rev. B **92**, 140411(R) (2015).

[23] R. J. Woolfson, G. A. Timco, A. Chiesa, I. J. Vitorica-Yrezabal, F. Tuna, T. Guidi, P. Santini, S. Carretta, and R. E. Winpenny (unpublished).

[24] E. Garlatti, S. Carretta, M. Affronte, E. C. Sañudo, G. Amoretti, and P. Santini, J. Phys. Condens. Matter **24**, 104006 (2012).

[25] E. Garlatti, S. Carretta, P. Santini, G. Amoretti, M. Mariani, A. Lascialfari, S. Sanna, K. Mason, J. Chang, P. Tasker, and E. K. Brechin, Phys. Rev. B **87**, 054409 (2013).

[26] P. Santini, S. Carretta, E. Liviotti, G. Amoretti, P. Carretta, M. Filibian, A. Lascialfari, and E. Micotti, Phys. Rev. Lett. **94**, 077203 (2005).

[27] I. Rousochatzakis, A. Läuchli, F. Borsa, and M. Luban, Phys. Rev. B **79**, 064421 (2009).

[28] A. Bianchi, S. Carretta, P. Santini, G. Amoretti, J. Lago, M. Corti, A. Lascialfari, P. Arosio, G. Timco, and R. E. P. Winpenny, Phys. Rev. B **82**, 134403 (2010).

[29] F. Borsa, A. Lascialfari, and Y. Furukawa, in *Novel NMR and EPR Techniques* (Springer, Berlin, Heidelberg, 2006).

[30] M. Belesi, A. Lascialfari, D. Procissi, Z. H. Jang, and F. Borsa, Phys. Rev. B **72**, 014440 (2005).

[31] S. H. Baek, M. Luban, A. Lascialfari, E. Micotti, Y. Furukawa, F. Borsa, J. van Slageren, and A. Cornia, Phys. Rev. B **70**, 134434 (2004).

[32] S. Carretta, P. Santini, G. Amoretti, M. Affronte, A. Candini, A. Ghirri, I. S. Tidmarsh, R. H. Laye, R. Shaw, and E. J. L. McInnes, Phys. Rev. Lett. **97**, 207201 (2006).

[33] In order to make the relaxation dynamics ergodic, we actually use slightly different magnetoelastic coupling constants for each Cr^{3+} ion, $\gamma_i \equiv \gamma + \delta_i$, with $\delta_i \ll \gamma$ a tiny random modulation. We have checked that the calculated $1/T_1$ curves do not appreciably depend on the presence and on the specific pattern of the δ_i constants. This indicates that in the investigated range of fields and temperatures, the relaxation pathways in the minimal model of Eq. (3) are sufficient to reproduce the dynamics of fluctuations about the equilibrium state probed by NMR.

[34] P. Santini, S. Carretta, E. Liviotti, and G. Amoretti, Physica B **374-375**, 109 (2006).

[35] G. Allodi, A. Banderini, R. D. Renzi, and C. Vignali, Rev. Sci. Instrum. **76**, 083911 (2005).

[36] A. G. Redfield, IBM J. **1**, 19 (1957).

[37] C. P. Slichter, *Principles of Magnetic Resonance* (Springer-Verlag, New York, 1992).

[38] The transverse relaxation rate $1/T_2$ contains also a temperature-independent contribution originating from the nuclear

dipole-dipole interaction among protons. At high temperatures, the electronic contribution to $1/T_2$ in Eq. (6) is small and only the nuclear dipole-dipole contribution survives. In fact, in the Cr_9 cluster $1/T_2$ is almost temperature independent at $T > 40$ K and thus we can take as a measure of the nuclear dipole-dipole contribution the experimental value of $1/T_2$ at $T = 100$ K.

[39] We have checked that a truncation of the molecule Hilbert space causes the relaxation rates to saturate at lower temperatures with respect to their real temperature dependence. Thus, in the temperature range above the peak in $(1/T_1)/(\chi T)$, relaxation rates are still too close to the Larmor frequency, leading to a slight overestimation of the calculated $1/T_1$ with respect to the experimental one.

[40] F. Adelnia, A. Chiesa, S. Bordignon, S. Carretta, A. Ghirri, A. Candini, C. Cervetti, M. Evangelisti, M. Affronte, I. Sheikin, R. Winpenny, G. Timco, F. Borsa, and A. Lascialfari, J. Chem. Phys. **143**, 244321 (2015).

[41] A. Abragam and B. Bleaney, *Electron Paramagnetic Resonance of Transition Ions* (Claredon Pres, Oxford, 1970).

[42] M. L. Baker, T. Guidi, S. Carretta, J. Ollivier, H. Mutka, H. U. Güdel, G. A. Timco, E. J. L. McInnes, G. Amoretti, R. E. P. Winpenny, and P. Santini, Nat. Phys. **8**, 906 (2012).

[43] G. Kamieniarz, P. Kozłowski, M. Antkowiak, P. Sobczak, T. Ślusarski, D. M. Tomecka, A. Barasiński, B. Brzostowski, A. Drzewiński, A. Bieńko, and J. Mroziński, Acta Phys. Pol. **121**, 992 (2012).

[44] R. A. Klemm and D. V. Efremov, Phys. Rev. B **77**, 184410 (2008).

[45] The simulation of $1/T_1$ and $1/T_2$ with our theoretical model is more time consuming when introducing a zero-field splitting term, since we can not no longer exploit the spherical symmetry of (1). Thus we have recalculated the temperature dependence of $(1/T_1)/(\chi T)$ only at low temperatures, where anisotropy effects are expected to be stronger.